Molecular Crystals and Liquid Crystals
Publication details, including instructions for authors and subscription information:
http://www.tandfonline.com/loi/gmcl16

Shear Viscosity Measurements in CBOOA

M. G. Kim [a b c], S. Park [a b], Sr. M. Cooper [a b] & S. V. Letcher [a b]

[a] Department of Physics, University of Rhode Island, Kingston, R.I., 02881

[b] Francis Bitter National Magnet Laboratory, MIT, Cambridge, Ma., 02134

[c] Agency for Defense Development, Seoul, Korea

Version of record first published: 29 Aug 2007.

To cite this article: M. G. Kim , S. Park , Sr. M. Cooper & S. V. Letcher (1976): Shear Viscosity Measurements in CBOOA, Molecular Crystals and Liquid Crystals, 36:1-2, 143-152

To link to this article: http://dx.doi.org/10.1080/00268947608084837

Mol. Cryst. Liq. Cryst., 1976, Vol. 36, pp. 143–152

Printed in Holland

Shear Viscosity Measurements in CBOOA†

M. G. KIM‡, S. PARK, Sr. M. COOPER and S. V. LETCHER

Department of Physics, University of Rhode Island, Kingston, R.I. 02881

and

Francis Bitter National Magnet Laboratory, MIT, Cambridge, Ma. 02134

(*Received May 11, 1976*)

The anisotropic shear viscosity of the liquid crystal CBOOA has been measured by observing the flow through a flat capillary. Uniform alignment was maintained by application of magnetic fields up to 85 kOe. In the nematic phase, five different measurements were made to determine the five independent coefficients. In the smectic phase, when the smectic planes were parallel to the capillary plates, the flow was nearly Newtonian and the temperature dependence had an Arrhenius behavior. When the smectic planes were parallel to the velocity and to the velocity gradient, the flow was non-Newtonian and rheopectic. This non-ideal behavior is attributed to the existence of nucleation of dislocations that can become pinned at the capillary walls.

Anisotropic shear viscosity coefficients of nematic liquid crystals have been measured by flow between parallel plates,[1–3] by couette flow,[4] by rotating the sample in a magnetic field (or equivalent),[5–9] by torsional shear flow,[10–11] and by acoustic shear impedometry.[12] Only in Ref. 2 has a complete set of the five coefficients been obtained in one experiment. Rotational viscosity techniques have also been applied to the smectic-C phase[13] and shear impedometry to smectic-A and B.[14] Continuum theory treatments of dissipative processes in nematics have been provided by Ericksen[15] and Leslie[16] and by Forster, *et al.*[17] and a generalized version applicable to smectics by Martin, *et al.*[18] We report here on capillary flow viscosity measurements in the nematic and smectic-A phases of *p*-cyanobenzylidene-*p*-*n*-octyloxyaniline (CBOOA) oriented in a magnetic field.

† Supported by National Science Foundation Grant GH-39313.
‡ Present address: Agency for Defense Development, Seoul, Korea.

EXPERIMENTAL

The rectangular aluminum capillary has dimensions 0.15 mm × 4.5 mm × 47 mm. A sample reservoir with width equal to that of the capillary is located at each end. A glass viewing tube allows observations of the liquid level. Applied gas pressure can partially cancel or reinforce the gravitational pressure head. The viscometer was immersed in an oil bath which could be placed in a strong magnetic field. Fields on the order of 20 kOe in the nematic and 50-70 kOe in the smectic were required to overcome the competing flow realignment.

The CBOOA sample was purchased from Eastman Kodak Company and was purified by recrystallization in *n*-heptane.

FLOW IN A FLAT CAPILLARY

Consider a centrally located slab of fluid of thickness $2x$ in a flat capillary of thickness t, width w, and length L. The force applied to this slab is $Pw2x$, where P is the applied pressure (gravitational head of the sample plus applied gas pressure) and the viscous force is $2\sigma wL$, where σ is the viscous stress. Then, in equilibrium, $\sigma = Px/L$. The stress vanishes at the center of the capillary ($x = 0$) and has a maximum value $\sigma_{max} = Pt/2L$ at the walls. The volume flow rate of fluid in the capillary is given by

$$\dot{Q} = \int_{-t/2}^{+t/2} v(x)w \, dx, \tag{1}$$

where v is the particle velocity. Integrating by parts, this becomes

$$\dot{Q} = \frac{2wL^2}{P^2} \int_0^{\sigma_{max}} \dot{\gamma}(\sigma)\sigma \, d\sigma, \tag{2}$$

where $\dot{\gamma} = -\partial v/\partial x$ is the shear strain rate.

For a Newtonian fluid, $\dot{\gamma} = \sigma/\eta_N$ and $\dot{Q} = Pwt^3/12L\eta_N$. Also, $\dot{Q} \propto -\dot{P}$, since P is just a measure of the liquid level in the viewing tube. The level decreases exponentially toward $P = 0$ with the time constant $\tau \propto \eta_N$. The proportionality constant is found by calibration and the time constant is found experimentally from the slope of the ln P vs. t curve.

RESULTS

A Nematic

Five different measurements are required to determine the five independent coefficients that describe the flow of an incompressible nematic. Our five measurements and the resulting Harvard coefficients[17] are given below.

1) Molecular axis normal to flow velocity and to the velocity gradient: $\eta_a = \nu_2$.

2) Molecular axis parallel to flow velocity: $\eta_b = \nu_3 + \gamma_1(1 - \lambda)^2/4$

3) Molecular axis parallel to velocity gradient: $\eta_c = \nu_3 + \gamma_1(1 + \lambda)^2/4$

4) Molecular axis in plane of and half way between velocity and velocity gradient vectors: $\eta_{45} = (2\nu_1 + 2\nu_2 + \gamma_1)/4$

5) Zero magnetic field, flow alignment angle θ_0:

$$\eta_0 = \eta_c \sin^2 \theta_0 + \eta_b \cos^2 \theta_0 + \alpha_1 \cos^2 \theta_0 \sin^2 \theta_0,$$

where

$$\alpha_1 = 2\nu_1 + 2\nu_2 - 4\nu_3 - \gamma_1\lambda^2$$

and where $\cos 2\theta_0 = 1/\lambda$.

In this notation, the ν_i's are flow viscosities, γ_1 is the orientational viscosity and λ is a dimensionless coupling coefficient.

The measured viscosities as a function of temperature are shown in Figure 1. The temperature dependences of η_c and η_a are Arrhenius with activation energies of about 7 kcal/mole and 12 kcal/mole, respectively. The viscosities η_b and η_{45} increase rapidly at low temperature due to pretransitional effects above the nematic-smectic A transition. The calculated Harvard coefficients are shown in Figure 2. Pretransitional divergence of γ_1 and ν_1 is seen, in qualitative agreement with the predictions of Jähnig and Brochard.[19]

At temperatures below 88°C, λ becomes less than unity, which means that the flow alignment in zero field is no longer stable[4] and relationship (5) above is no longer valid. This is consistent with earlier observations in CBOOA and some other materials.[2–4]

B Smectic

Prior to each series of smectic measurements, the magnetic field was applied in the nematic phase and the sample was then cooled to the smectic.

1) Magnetic field perpendicular to the velocity and velocity gradient. In this orientation, the smectic planes are parallel to the flow velocity and to

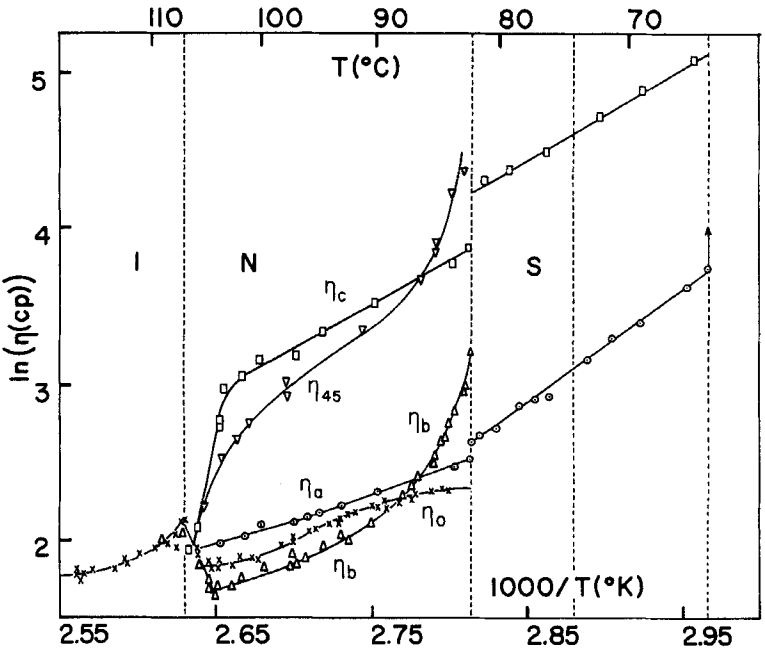

FIGURE 1 Measured viscosities of CBOOA as a function of 1000/T. Five different measurements are shown in the nematic (N) and two in the smectic (S). The smectic phase supercooled to about 65°C.

the velocity gradient. The capillary surfaces were not treated in any way to induce surface alignment. The following behavior was observed:

a) Repeated measurements at a given field and temperature were not reproducible unless they were preceded by a rather vigorous flow of the sample back and forth through the capillary. If that procedure was followed, the results were repeatable and the measured viscosity had the minimum value for that temperature and field. In general, the longer the time that elapsed between a measurement and a preceding flow, the larger the measured viscosity. For example, at 79°C and 56.6 kOe, a fifteen minute delay between successive measurements resulted in a 15–20% increase in the apparent viscosity.

b) The flow was non-Newtonian; i.e., the ln P *vs.* t curve was not linear. See the top curve of Figure 3. This behavior is distinct from the time dependence just mentioned. The following procedure was adopted to obtain the data in Figure 3 and all other data for this orientation of smectic. From an initial pressure (180 mmH_2O in Figure 3), intermediate times were measured for a total reduction of liquid level of 25 mm. The sample was then run back

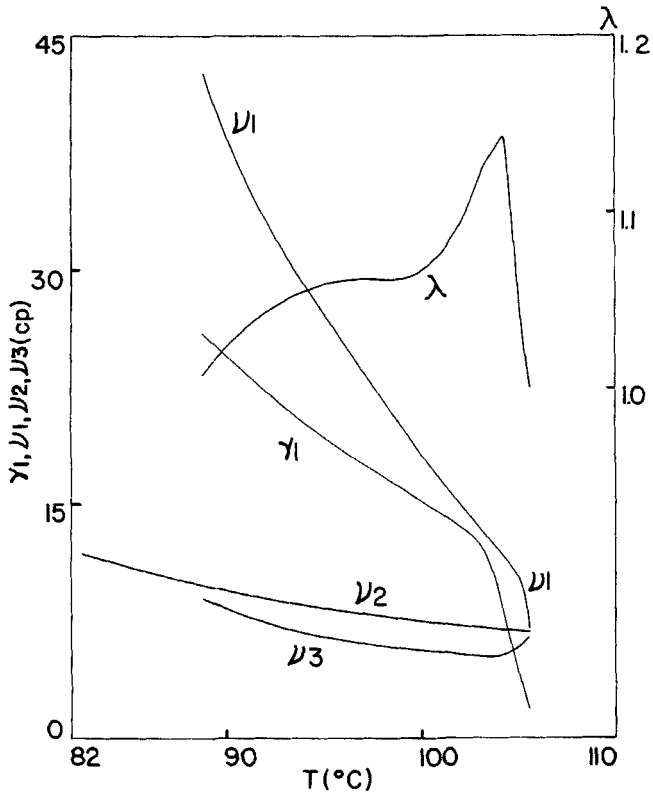

FIGURE 2 Calculated viscosities in nematic CBOOA. The high temperature points of λ (above 104°C) are not reliable because of the subtraction of nearly equal measured viscosities.

and forth through the capillary and the procedure was repeated with a lower initial pressure. This was repeated for a series of overlapping pressures. Extrapolation to zero time for sets with high initial pressures yielded lower time constants than those with lower initial pressures. Figure 3 includes some time-dependent behavior (non-overlapping portions of a set varied from ~ 20 sec to ~ 300 sec), but the main effect depicted is the pressure dependence.

This non-Newtonian behavior must fall somewhere between the rheological extremes of a pseudoplastic with no yield stress (curve A of Figure 4) and a Bingham plastic (represented by $\sigma - \psi = \eta\dot{\gamma}$; curve C of Figure 4).[20] Curve B represents the intermediate case of a pseudoplastic with a yield stress. We find that our ln P vs. t plots can be made nearly linear over the measured range of pressures by renormalizing the pressure, such that $P - P' = (P_0 - P')e^{-t/\tau}$ and then $\dot{P} = -\tau^{-1}(P - P')$. That this behavior is phenomenologically equivalent to that of a Bingham plastic can be seen by using

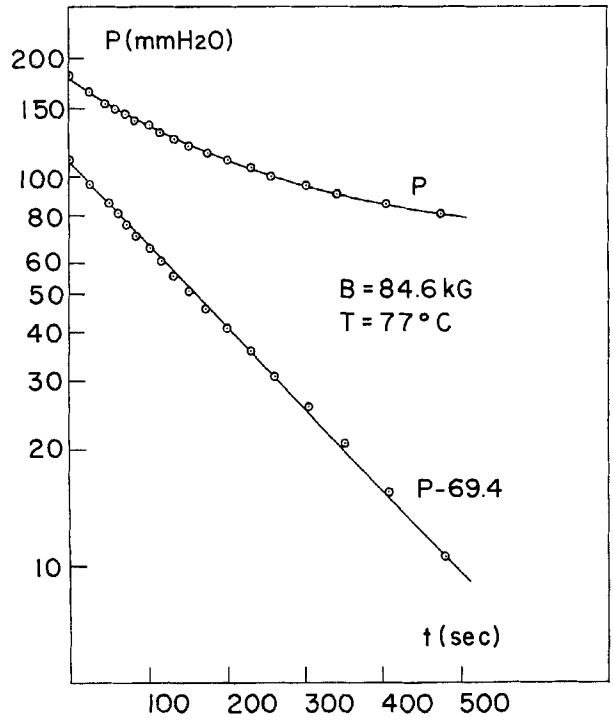

FIGURE 3 Top curve shows measured pressure in units of mm of H_2O (changes of pressure are the same as change of the liquid level) as a function of temperature. Bottom curve shows the same data when pressure has been renormalized by subtracting 69.4 mmH_2O.

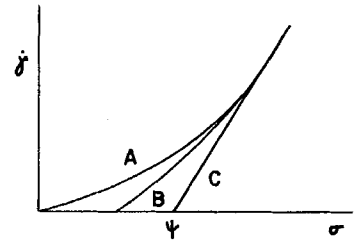

FIGURE 4 Some possible stress (σ)—strain rate ($\dot{\gamma}$) relationships for non-Newtonian fluids; pseudoplastic (A), pseusoplastic with a yield stress (B), Bingham plastic (C).

Eq. (2) to calculate the volume flow rate for a Bingham body in a flat capillary. Thus, $\dot{Q} = (wt^2/6\eta)(\sigma_{max} - 3\psi/2)$ and $\dot{P} \propto \eta^{-1}(P - a\psi)$, where a is a geometrical constant. Then $\tau(\propto \eta)$ is constant and corresponds to the infinite-flow-rate limit of the viscosity. The calculated values of P' (or ψ) that gave the best linear fit were relatively temperature independent at 75 mmH_2O (8 dyne/cm^2) below about 73°C and decreased rapidly at higher temperatures to 30 mmH_2O (3 dyne/cm^2) at 82°C.

c) The infinite-flow-rate limit of viscosity as a function of temperature exhibits Arrhenius behavior. This is shown in Figure 1, where the data referring to this orientation of the smectic were taken at $B = 84.6$ kOe. The activation energy is about 12 kcal/mole.

2) Magnetic field parallel to the velocity gradient.

A thin film of lecithin was applied to the capillary walls to assist the alignment, which is characterized by the smectic planes being parallel to the walls. Because of the higher viscosity, the measurements were made at higher

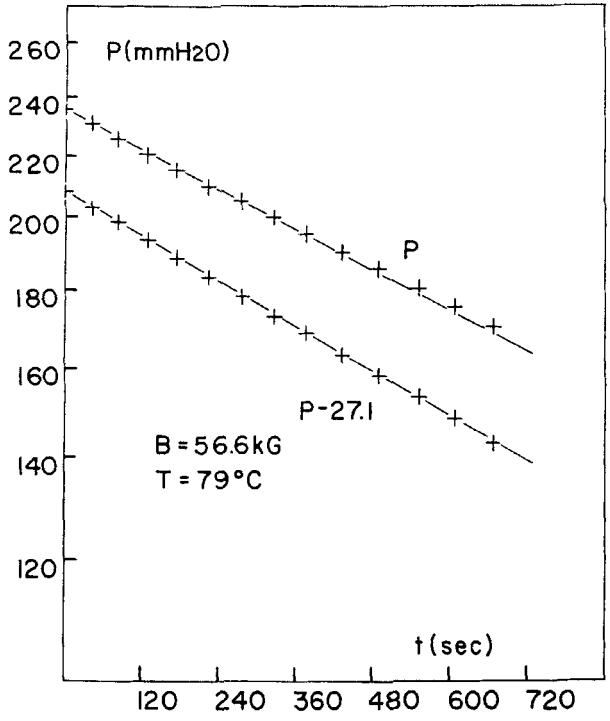

FIGURE 5 Top curve shows measured pressure as function of time in smectic phase of CBOOA at $T = 79$°C and $B(=56.6$ kOe) parallel to the velocity gradient. Slightly renormalized data are shown in the lower curve.

applied pressures and the flow generally was measured over longer time intervals than in the previous case. In spite of this the flow was nearly Newtonian; only a slight pressure and/or time dependence was observed. In the top curves of Figure 5, ln P *vs.* t at 79°C is seen to be nearly linear. The renormalization constant P' is 27.1 mmH_2O, or 12% of the initial pressure. Running the sample back and forth through the capillary prior to a measurement generally had a negligible effect on the result. The temperature dependence of viscosity at 56 kOe shown in Figure 1, is approximately Arrhenius with an activation energy of 10–15 kcal/mole.

3) Magnetic field parallel to flow velocity.

The smectic planes here were normal to the flow velocity and the only flow in a defect-free sample would be the permeation of molecules through the planar structure.[21] We have observed the flow for this orientation in both a narrow flat capillary and a large (5 mm ID) round capillary. In each case the flow is characterized by shear thinning. Typically, the apparent viscosity increases initially and then levels off and a repetition of the experiment by raising the liquid level and letting it fall again results in an order of magnitude decrease in the apparent viscosity. This suggests that the flow is controlled by defect nucleation at the capillary walls as proposed by de Gennes.[22]

DISCUSSION

In the nematic phase our values of γ_1 are smaller than those obtained by Hardouin, *et al.* in a rotating field experiment[8] and by Huang, *et al.*[22a] Similarly, the values of γ_1 for MBBA and HBAB obtained by Gähwiller[2] in a capillary flow experiment are smaller than the corresponding rotating field measurements of Gasparoux and Prost[7] and Meiboom and Hewitt.[9] The reason for this is not clear, although it has been suggested[9] that the existence of inversion walls or other imperfections plays a role.

For orientations (1) and (2) of the smectic phase, the viscosity was nearly continuous with the nematic viscosity at the A–N transition, with an increase of activation energy in the smectic that reflects the restrictions on the freedom of motion of the molecules in the smectic phase.

A perfectly aligned smectic single crystal has sufficiently simple structure that it would be expected to exhibit Newtonian flow behavior. One would expect then that the anomalous behavior apparent in orientation (1) is due to a defect structure. The existence of dislocations in a smectic-A material has been discussed by several authors.[23–28] It is proposed here that some of the flow properties described can be attributed to the existence and, especially, to the pinning of dislocations. In orientation (1), an edge dislocation would be normal to the capillary walls, as in Figure 6. In the absence of large amounts

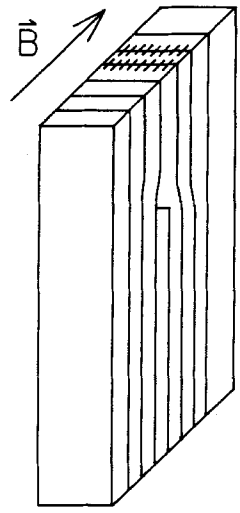

FIGURE 6 Configuration of an edge dislocation in a smectic A when the orienting field is parallel to the capillary walls.

of impurities, one would expect most of the dislocations to be pinned at the rough surfaces of the capillary walls.

Vigorous flow prior to a measurement will free the dislocations from their pinning sites and provide a lower measured viscosity. The critical tensile stress required to cause unstable growth of pinned dislocations has been estimated[25] to be $\sigma_c \sim 2ba/t$, where b is the elastic constant for compression of the smectic layers, a is the interlayer distance and t is the dislocation length. If we take $b \sim 10^8$ dyne/cm^2, $a \sim 20 \times 10^{-8}$ cm, and $t \sim 1.5 \times 10^{-2}$ cm, then $\sigma_c \sim 2.5 \times 10^2$ dyne/cm^2. We assume that the critical stress for climb motion due to a shear stress is of the same order of magnitude. (Climb has been shown to be somewhat easier than glide in smectics[23a].) A typical stress during a measurement is given by $\sigma_{max} = Pt/2L$, where $P \sim 150$ mm$H_2O \sim 1.5 \times 10^4$ dyne/cm^2, $t \sim 1.5 \times 10^{-2}$ cm, $L \sim 4.7$ cm, and $\sigma_{max} \sim 24$ dyne/cm^2, far below the critical stress. On the other hand, the vigorous flow preceding a measurement is typically provided by a pressure of about $20\text{–}30 \times 10^4$ dyne/cm^2, which corresponds to a σ_{max} of the same order of magnitude as the critical stress.

Following a vigorous flow, an array of pinned dislocations would gradually reestablish itself. Presumably a large number of unpinned dislocations would be present due to the rapid flow. Dislocations might also diffuse into the capillary region or, if the fluid is gently flowing as in a measurement, continue to be generated at the entrance and exit to the capillary or at the capillary walls. In orientation (2), edge dislocations are parallel to the capillary walls

and would not be expected to be pinned by the boundaries of the capillary. This simple model is then consistent with the observed time and history dependence of the viscosity.

The nature and source of the non-Newtonian behavior of orientation (1) is less clear. It is assumed that the measurements represented in the top curve of Figure 3 were made sufficiently soon after the vigorous flow that pinning has not been reestablished. Although the data have been fit to a Bingham behavior to obtain the bottom curve of Figure 3 and the high-flow-rate limit shown in Figure 1, extrapolation of the Bingham behavior into the low-flow-rate region is at least doubtful. It is not clear, for example, what would be the cause of a yield stress in a fluid with unpinned dislocations. The data in Figure 3 can also be fit fairly well to a power-law pseudoplastic behavior ($\sigma^m = k\dot{\gamma}$), with exponent $m \simeq 2.7$. Further measurements at lower applied stresses are needed to establish the complete flow behavior.

References

1. M. Miesowicz, *Nature* **158**, 27 (1946).
2. Ch. Gähwiller, *Mol. Cryst. Liq. Cryst.* **20**, 301 (1973).
3. P. Pieranski and E. Guyon, *Phys. Rev. Letters* **32**, 924 (1974).
4. P. E. Cladis and S. Torza, *Phys. Rev. Letters* **35**, 1283 (1975).
5. V. N. Tsvetkov, *Acta Physicochem. U.R.S.S.* **10**, 555 (1939).
6. J. Prost and H. Gasparoux, *Phys. Lett.* **36A**, 245 (1971).
7. H. Gasparoux and J. Prost, *J. de Phys.* **32**, 953 (1971).
8. F. Hardouin, M. F. Archard, and H. Gasparoux, *Solid State Comm.* **14**, 453 (1974).
9. S. Meiboom and R. C. Hewitt, *Phys. Rev. Letters* **30**, 261 (1973).
10. J. Wahl and F. Fischer, *Mol. Cryst. Liq. Cryst.* **22**, 359 (1973).
11. T. Walterman and F. Fischer, *Z. Naturforsch.* **30a**, 519 (1975).
12. P. Martinoty and S. Candau, *Mol. Cryst. Liq. Cryst.* **14**, 293 (1971).
13. S. Meiboom and R. C. Hewitt, *Phys. Rev. Letters* **34**, 1146 (1975).
14. Y. Thiriet and P. Martinoty, *J. de Phys. Lett.* **36**, L-125 (1975).
15. J. L. Ericksen, *Arch. Rat. Mech. Anal.* **4**, 231 (1960).
16. F. M. Leslie, *Arch. Rat. Mech. Anal.* **28**, 265 (1968).
17. D. Forster, T. C. Lubensky, P. C. Martin, J. Swift, and P. S. Pershan, *Phys. Rev. Letters* **26**, 1016 (1971).
18. P. C. Martin, O. Parodi, and P. S. Pershan, *Phys. Rev.* **A6**, 2401 (1972).
19. F. Jähnig and F. Brochard, *J. de Phys.* **35**, 301 (1974).
20. E. C. Bingham and H. Green, *Proc. ASTM* **19**, 640 (1919); see also, e.g., A. G. Frederickson, *Principles and Applications of Rheology* (Prentice-Hall, Englewood Cliffs, N.J. 1964).
21. W. Helfrich, *Phys. Rev. Letters* **23**, 372 (1969).
22. P. G. de Gennes, *Phys. Fluids* **17**, 1645 (1974).

22a. C. Huang, R. S. Pindak, P. J. Flanders, and J. T. Ho, *Phys. Rev. Letters* **33**, 400 (1974).

23. P. S. Pershan, *J. Appl. Phys.* **45**, 1590 (1974); C. E. Williams and M. Kleman, *J. de Phys. Lett.* **35**, L33 (1974); *J. de Phys.* **36**, Cl-315 (1975).

23a. C. E. Williams and M. Kleman, *J. de Phys. Lett.* **35**, L49 (1974).

24. Orsay Group on Liquid Crystals, *J. de Phys.* **36**, Cl-305 (1975).
25. P. S. Pershan and J. Prost, *J. Appl. Phys.* **46**, 2343 (1975).
26. N. A. Clark and R. B. Meyer, *Appl. Phys. Letters* **22**, 493 (1973).